Journal of African Earth Sciences 153 (2019) 208–218

Contents lists available at ScienceDirect

Journal of African Earth Sciences

journal homepage: www.elsevier.com/locate/jafrearsci

Geochemistry and provenance of Neoproterozoic metasedimentary rocks from the Togo structural unit, Southeastern Ghana

C.Y. Anani[a,*], S. Bonsu[b], D. Kwayisi[a,c], D.K. Asiedu[a]

[a] Department of Earth Science, University of Ghana, P.O. Box LG 58, Legon-Accra, Ghana
[b] Ghana Geological Survey Authority, P.O. Box M80, Accra, Ghana
[c] Department of Geology, University of Johannesburg, APK campus, Johannesburg, South Africa

ARTICLE INFO

Keywords:
Neoproterozoic
Geochemistry
Provenance
Tectonic setting
Togo structural unit
Ghana

ABSTRACT

Neoproterozoic metasedimentary rocks of greenshist facies, consisting predominantly of quartzites, phyllites, and phyllonites, occur in the Akwapim range of the Togo Structural Unit (TSU) in Ghana. The geochemistry of the phyllites were studied to determine their provenance and tectonic setting. The major element analysis was carried out by the Inductively Coupled Plasma-Atomic Emission Spectroscopy (ICP-AES) and trace elements, including REEs, by the Inductively Coupled Plasma-Mass Spectroscopy (ICP-MS) method. The studied metasedimentary rocks have SiO_2 and Al_2O_3 contents comparable to that of average Neoproterozoic upper crust. The metasedimentary rocks are strongly depleted in CaO, Na_2O, and Sr and enriched in K_2O, Ba and Rb with respect to average Neoproterozoic upper crust, reflecting K addition during diagenesis. Zr and Hf concentrations are significantly above Neoproterozoic upper crustal values. Chondrite-normalized rare earth element (REE) patterns are characterised by fractionated light-REE (LREE) (average La_N/Sm_N = 3.68), significant negative europium anomaly (average Eu/Eu* = 0.61) and fairly flat heavy-REE (HREE) (average Gd_N/Yb_N = 1.3). The geochemical data, particularly the high La/Sc, Th/Sc, La/Co, Th/Co, Zr/Sc, La/Th ratios, Eu/Eu* values, and high Zr and Hf concentrations, suggest that the metasedimentary rocks of the Togo Structural Units in the Akwapim range were derived mainly from recycled sedimentary sources. Comparison of geochemical signatures of the studied metasedimentary rocks with those of the Paleoproterozoic Birimian rocks suggests that the felsic materials in the Togo Structural Units (TSU) could not have been derived predominantly from the Birimian rocks, implying more distal sources. The studied metasedimentary rocks exhibit provenance characteristics similar to that of the Kwahu/Bombouaka Group of the Voltaian Basin, suggesting derivation from the same source, probably in the Amazon Craton. The metasedimentary rocks exhibit geochemical characteristics indicative of sediments derived from a passive continental margin. This inference supports previous studies that indicate that prior to the Pan-African Dahomeyide orogenic event, the southern margin of the West African Craton (WAC) was under passive margin settings.

1. Introduction

The Pan-African Dahomeyide orogenic belt occupies an approximately 1000 km long stretch from the southeastern Ghana, through Togo, Benin to Nigeria (Attoh, 1998; Attoh and Nude, 2008). It forms part of the very long (> 2500 km) Trans-Saharan mobile belt which formed during the Pan-African orogenic event. The Pan-African Dahomeyide orogenic belt comprises three structural units. From west to east, these are the Buem, the Togo and the Dahomeyan structural units (Fig. 1). The Togo Structural Unit (TSU) is an irregular, fault-bounded belt of metamorphic units that comprise the series of hills and ridges, which start from just west, and north of Accra, extending along the Ghana-Togo border and into northern Benin where it is called the Atacora Range (Adjei, 1968; Adjei and Tetteh, 1997; Junner, 1940). Prominent among these hills and mountains are the Akuapim range, which comprises cataclastic quartzites interbedded with phyllites (Junner, 1940; Junner and Hirst, 1946; Junner and Service, 1936).

The chemical composition of fine-grained sedimentary rocks is particularly valuable for provenance studies as they provide a representative view of the average crust in the area due to their grain size homogeneity and post-depositional impermeability (Cox and Lowe, 1995; Taylor and McLennan, 1985). Chemical composition can be extracted by whole-rock mineralogical and geochemical analyses of the sediments (Taylor and McLennan, 1985). These analyses determine the

* Corresponding author.
E-mail address: cyanani@ug.edu.gh (C.Y. Anani).

https://doi.org/10.1016/j.jafrearsci.2019.03.002
Received 20 February 2018; Received in revised form 12 February 2019; Accepted 5 March 2019
Available online 11 March 2019
1464-343X/

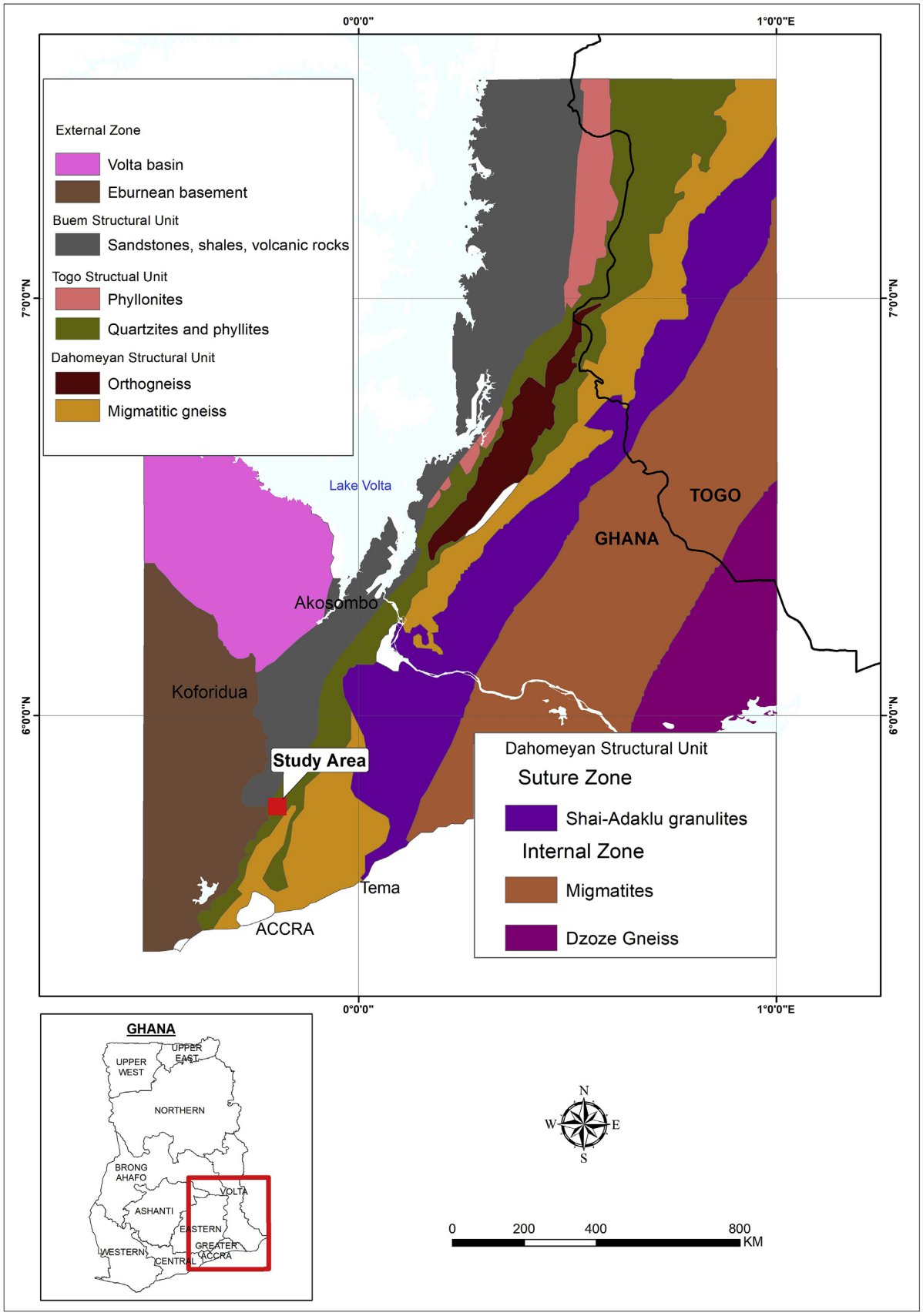

Fig. 1. Generalized tectono-stratigraphic map of south eastern Ghana showing the study area (modified from Osae et al., 2006).

mineralogical content as well as the major and trace element (including REEs) abundances, which give significant evidence used in constraining the source-area weathering, source rocks and tectonic setting of sedimentary and metasedimentary rocks.

Although the chemical composition of sedimentary and metasedimentary rocks is very useful in deciphering their provenance and tectonic setting, studies on the Togo Structural unit is devoid of its application. The chemical characteristics of the rocks of the Togo Structural unit have so far, not been applied to constrain their provenance and the tectonic setting.. Various workers have suggested that the Togo Structural unit can be correlated to the Lower Member of the Voltaian Supergroup. According to Kalsbeek et al. (2008); Kalsbeek and Frei (2010), Lead-lead dating of detrital zircons obtained within the quartzites of the Togo Structural Unit help buttress this opinion. Indeed, zircon age distributions are comparable to those of Kwahu/Bombouaka Group of the Voltaian Basin (Kalsbeek et al., 2008). However, there are no geochemical studies to put better constraint of the provenance, source area lithology and tectonic setting of the Togo Structural unit. Hence, this study presents the mineralogical and geochemical studies of the Togo phyllites to determine the source-area lithology, as well as constrain the tectonic setting and provenance.

2. Geological setting

The West African Craton (WAC) according to Ennih and Liégeois (2008), became tectonically stable since the last major stage of the Eburnean orogenesis at 2000 Ma and comprising two major basement domains. These are the Reguibet domain to the north and the Leo-Man shield to the south. The domains are of Archean and Paleoproterozoic age and are separated by Neoproterozoic to Paleozoic sedimentary cover of taoudeni (Doblas et al., 2002). Hoffman (1991); Dalziel (1991), (1997); Weil et al. (1998) have hypothesised in their reconstruction of the supercontinent Rodinia that they assembled around 1000–1200 Ma ago and that the West-African craton was situated close to the Amazonian craton. Nevertheless, in contrast to the WAC, the Amazonian craton had undergone several cycles of late Palaeoproterozoic and Mesoproterozoic orogenic activity, and therefore rocks with age ranges between 1000 and 2000 Ma are common (e.g. Santos et al., 2000; Tassinari et al., 2000; Ganade deAraujo et al., 2016). The WAC is surrounded on all its margin by Pan-African mobile belts. To the north by the Anti-Atlas belt (Hefferan et al., 2000; Ennih and Liégeois, 2001), to the south, the Rockelides and the Bassarides belts and to the west, the Mauritanides belt (Villenenve and Dallmeyer, 1987) and east by the Trans-Saharan belt (Black et al., 1979, 1994; Affaton et al., 1991; Attoh and Nude, 2008). The southeastern portion of the Trans-Saharan mobile belt is exposed in Ghana, Togo and Benin republics as the Dahomeyide belt. The Dahomeyide belt is categorized into three structural units namely; the Dahomeyan, Togo and Buem Structural units. These belts are bounded by thrust contacts.

The area of investigation is situated in the Akwapim range in the southeastern part of Ghana (Fig. 1). The Akuapim range falls under the Togo Structural Unit, which forms part of the Dahomeyide belt of Ghana. The Dahomeyide belt, which is part of the Pan-African orogenic belt, is believed to have resulted from the breakup of Rodinia supercontinent which led to the assemblage of cratonic material on the northwestern part of the Gondwana supercontinent (Cordani et al., 2003; Hoffman, 1991). The Togo Structural Unit is bordered to the west by the Cape Coast granitoid complex rocks, the Voltaian Basin and the Buem Structural Unit (Duodu, 2009, Fig. 1). On the eastern section of the Togo Structural Unit are the Devonian Accraian rocks and Dahomeyan metamorphic basement rocks. The Togo Structural Unit consists of quartz sericite-schists, quartzites, phyllites and chlorite schist (Adjei and Tetteh, 1997; Grant, 1969; Junner and Hirst, 1946; Robertson, 1925). Hornstones, jaspers and hematite quartz-schists occur as post-depositional rocks within the unit (Junner and Service, 1936).

Rocks in the Togo units generally strike northeast and dip in the southeastern direction. Adjei and Tetteh (1997) described the quartzites and phyllites within the Togo units are intensely deformed with deformation generally occurring as craton recumbent folds with pervasive sub-horizontal foliation. The earliest folds in the Togo units are the recumbent folds, with isoclinal to open folds occurring later (Adjei and Tetteh, 1997). The degree of metamorphism and deformation within the quartzites increases towards the southeast (Wright et al., 1985). Ahmed et al. (1977) indicated that the Togo Structural Unit comprises cataclastic quartzites interbedded with phyllites. The cataclastic quartzites are the predominant members of the unit. They are generally grey, medium to fine-grained, thickly foliated with joints and micro-fractures. The phyllites underlie the quartzites and are mostly composed of mica and chlorite. They are mostly fine-grained, thinly foliated with joints and micro-fractures. Folds, which occur within the quartzites and phyllites, are predominantly isoclinal with axial planes inclined to southeast at 30° to 60° and minor recumbent folds with a general dip of less than 30° (Kesse, 1985).

The Togo structural unit, according to Griffis et al. (2002), marks the western limits of a very large area affected by the Pan-African orogenic event that peaked at about 600-550 Ma and whose effects extend right across Nigeria.

3. Materials and methods

Outcrops of phyllites were sampled for their whole-rock geochemical compositions (Fig. 2). Samples showing visible quartz veinlets, which clearly represent remobilization, were avoided for the analysis. In all, thirty (30) samples were selected for the whole-rock geochemical analysis, at the ALS laboratory in Vancouver, Canada.

The major elements were analysed by the Inductively Coupled Plasma-Atomic Emission Spectroscopy (ICP-AES) method. About 0.200g of prepared sample was fused with lithium metaborate in a furnace at 1025 °C. The melt product was then allowed to cool. This was then dissolved in an acid mixture consisting of nitric (HNO_3), hydrochloric (HCl) and hydrofluoric (HF) acids. The final solution was then analysed for the major element composition using the ICP-AES with a precision better than 3%. The Inductively Coupled Plasma-Mass Spectroscopy (ICP-MS) method was used for the trace elements analyses with a precision of about 5%. The analyses were done by lithium borate fusion of prepared sample weighing 0.100g the protocols observed for the major element analyses were also observed. The base metals were analysed using the ICP-AES. A 0.25g prepared sample was digested with perchloric, nitric, hydrofluoric and hydrochloric acids. Dilute hydrochloric acid was then added to the residue and the solution was analysed by the ICP-AES at ± 5% precision. Results obtained were corrected for spectral inter-element interferences (ALS laboratory).

4. Geochemical results

4.1. Major elements

The analysed metasedimentary rocks of the Togo Structural Unit show wide variations in the major element compositions (Table 1), particularly for their SiO_2 (52.6–94.1 wt%), Al_2O_3 (3.08–20.41 wt%), and K_2O (0.77–6.38 wt %) contents. The TiO_2 (0.12–1.06 wt %), MnO (< 0.01 wt %), MgO (0.07–1.75 wt %), CaO (0.01–0.17 wt %), Na_2O (0.01–0.46 wt %) and P_2O_5 (0.01–0.1 wt %) contents are generally low.

The relationship between SiO_2 and the other major elements is shown in Fig. 3. SiO_2 show strong or moderate negative correlation with the following major oxides: Al_2O_3 (correlation coefficient, $r = -0.92$), TiO_2 ($r = -0.90$), Fe_2O_3 ($r = -0.75$), MgO ($r = -0.75$), K_2O ($r = -0.76$), Na_2O ($r = -0.68$) and P_2O_5 ($r = -0.67$). MnO and CaO do not show any variation with SiO_2. The major oxides TiO_2 ($r = 9.72$), MgO ($r = 0.58$), Na_2O ($r = 0.77$), and K_2O ($r = 0.85$) show positive correlations with Al_2O_3 and suggest that these elements are associated mainly with aluminous clay minerals such as illite, and

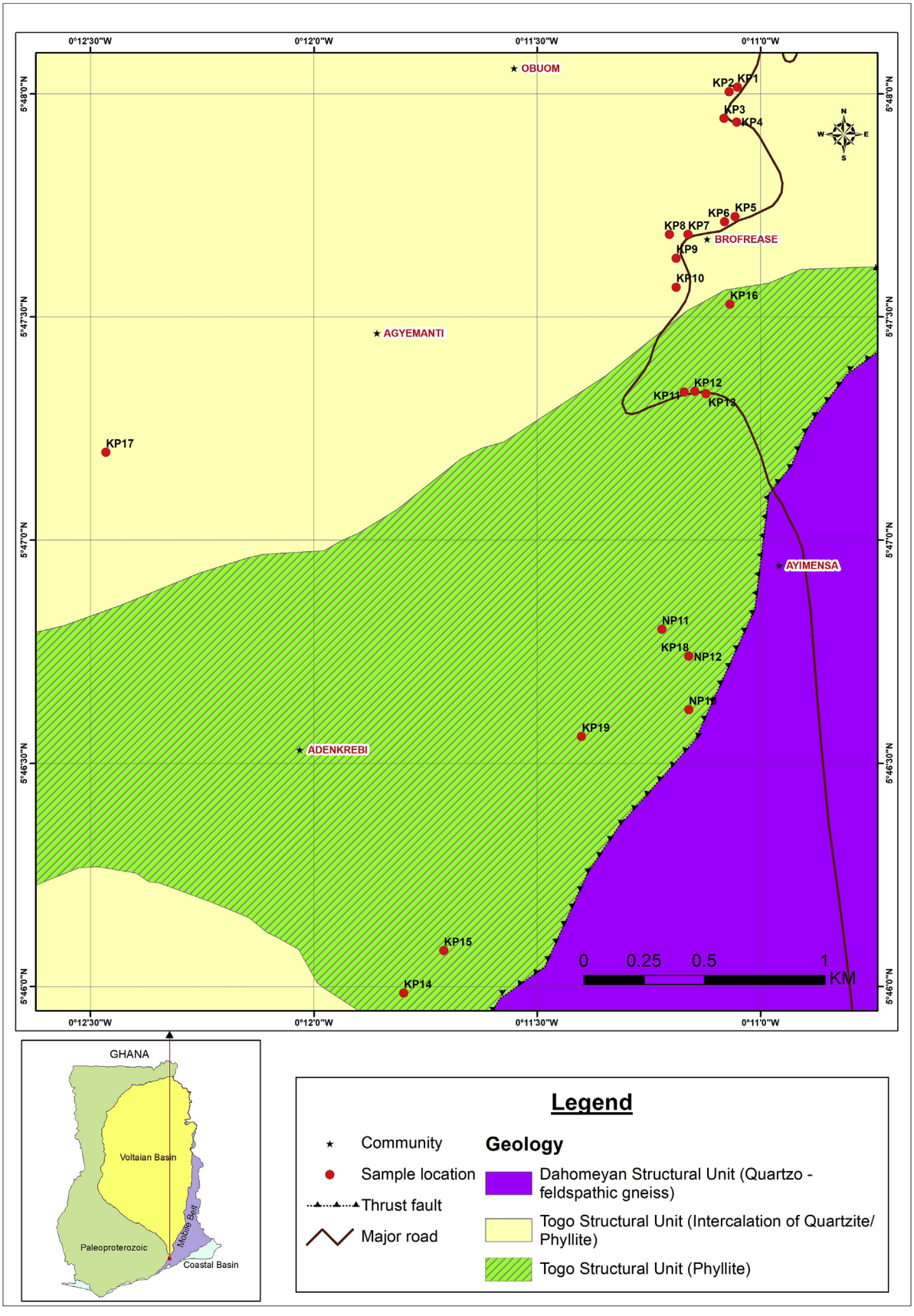

Fig. 2. Geological map of the study area showing the sample locations (modified from Duodu, 2009).

Table 1
Major, trace, and rare earth element analyses of TSU metasedimentary rocks.

Sample	KP1A	KP2A	KP3A	KP4A	KP5A	KP6A	KP7A	KP8A	KP9A	KP10A	KP11A	KP11B	KP12A	KP13A	KP14A
SiO_2	68.8	62.3	71.5	93.4	90.5	86.7	82.3	52.6	90.4	94.1	70.7	73.4	79	76.8	77.2
TiO_2	1.06	0.99	0.90	0.20	0.17	0.35	0.45	0.77	0.20	0.12	0.70	0.71	0.54	0.56	0.63
Al_2O_3	20.1	19.7	18.0	4.92	4.75	7.46	8.30	15.3	4.57	3.08	16.1	13.6	12.0	12.2	13.1
Fe_2O_3	0.81	4.04	1.40	0.41	0.42	2.19	4.06	14.0	1.85	1.28	2.57	2.65	1.37	1.40	1.70
MnO	0.01	0.01	0.01	0.01	0.01	0.01	0.01	0.77	0.01	0.01	0.01	0.01	0.01	0.01	0.01
MgO	0.21	1.28	0.62	0.16	0.16	0.11	0.12	1.66	0.29	0.07	1.08	0.85	0.71	0.73	0.88
CaO	0.02	0.02	0.01	0.01	0.01	0.01	0.01	0.17	0.01	0.01	0.01	0.01	0.01	0.01	0.01
Na_2O	0.46	0.10	0.12	0.02	0.01	0.06	0.07	0.14	0.02	0.01	0.08	0.06	0.05	0.05	0.08
K_2O	4.74	6.38	5.04	1.39	1.39	2.05	2.34	4.00	1.11	0.77	5.61	4.67	4.29	4.51	4.39
P_2O_5	0.03	0.02	0.01	0.01	0.01	0.01	0.02	0.10	0.01	0.01	0.01	0.01	0.01	0.01	0.01
LOI	3.43	3.93	3.36	1.08	1.10	1.60	1.98	8.88	1.17	1.10	3.09	2.69	2.21	2.24	2.51
Total	96.24	94.79	97.56	100.53	97.43	98.95	97.68	89.41	98.47	99.46	96.87	95.92	97.99	96.28	98.01
Rb	154	210	165	41.4	41.6	63.8	68.1	127	35.4	24	159	137	118	120	125
Sr	205	33.5	46.9	11.6	10.6	37.0	44.3	82.7	13.5	9.50	24.7	20.6	13.8	14.2	18.4
Ba	1575	1165	945	228	223	411	437	777	281	156	978	843	755	775	759
Y	33.2	47.8	34.4	14.4	13.4	19.1	27.8	39.4	11.6	10.0	26.7	24.9	16.3	17.2	24.7
Zr	479	559	460	407	331	542	594	285	271	274	406	468	378	387	571
Hf	12.3	14.7	11.8	10.0	8.40	13.2	15.3	7.70	7.10	6.60	10.5	12.0	9.80	9.90	14.8
Nb	20.0	18.2	18.3	4.60	4.20	7.00	8.80	15.4	4.00	2.70	13.6	14.2	9.70	10.0	12.4
Ta	1.40	1.30	1.30	0.30	0.30	0.50	0.60	1.10	0.30	0.20	0.90	1.00	0.70	0.70	0.80
Th	18.6	17	17.4	4.73	4.21	6.85	9.83	16.8	4.39	2.84	13	13.6	9.43	9.84	12.5
U	3.92	5.06	4.69	1.67	1.52	2.95	2.8	4.21	1.28	1.14	3.36	3.45	3.05	3.13	3.13
Sc	14	16	14	3	3	5	7	14	3	3	12	10	10	11	10
V	115	118	90	17	17	28	36	106	19	15	80	61	65	69	58
Cr	90	70	60	20	20	30	40	60	20	10	40	40	40	40	40
Co	1	3	1	1	1	2	5	25	5	2	4	3	4	4	3
Ni	5	10	11	5	7	5	9	24	14	14	7	8	11	10	8
Cu	3	10	2	4	4	10	23	5	6	12	17	11	5	5	7
La	50.8	30.9	41.7	18.2	16.9	22.7	31.5	44.9	19.4	10.7	36.9	34.9	23.6	24.3	31.5
Ce	99.8	69.7	81.4	41.0	39.0	52.5	73.1	94.8	37.4	24.3	75.1	71.5	50.1	51.2	66.2
Pr	10.4	7.71	9.11	4.94	4.59	5.97	8.27	10.5	4.12	2.94	8.34	7.84	5.43	5.46	7.31
Nd	35.8	30.2	34.0	18.6	18.4	23.8	33.1	42.0	15.9	12.2	30.7	29.0	19.7	20.8	28.5
Sm	6.11	6.66	6.62	3.9	3.43	4.77	6.04	8.69	2.85	2.54	5.41	5.21	3.45	3.39	5.24
Eu	1.16	1.31	1.21	0.57	0.58	0.78	1.20	1.60	0.54	0.43	0.97	0.87	0.58	0.61	0.95
Gd	4.86	6.78	5.61	3.15	2.75	3.39	5.06	7.91	2.28	1.87	4.34	3.69	2.57	2.68	4.11
Tb	0.86	1.28	0.92	0.41	0.43	0.52	0.79	1.16	0.32	0.30	0.74	0.64	0.41	0.43	0.66
Dy	6.02	8.46	6.12	2.63	2.48	3.35	5.17	7.35	2.15	1.78	4.97	4.41	2.92	3.01	4.55
Ho	1.22	1.82	1.27	0.53	0.54	0.68	1.05	1.42	0.44	0.38	1.06	0.95	0.62	0.67	0.96
Er	3.64	5.56	3.85	1.66	1.41	2.02	2.78	4.27	1.32	1.05	2.96	2.83	2.18	2.32	2.87
Tm	0.54	0.77	0.57	0.25	0.18	0.32	0.43	0.55	0.19	0.16	0.47	0.44	0.31	0.33	0.44
Yb	3.75	5.12	3.86	1.44	1.41	2.23	2.94	3.96	1.48	1.06	3.30	3.11	2.28	2.51	3.14
Lu	0.60	0.73	0.60	0.27	0.23	0.34	0.45	0.58	0.22	0.16	0.48	0.49	0.37	0.39	0.49
Eu/Eu*	0.65	0.60	0.61	0.50	0.58	0.59	0.66	0.59	0.65	0.60	0.61	0.61	0.60	0.62	0.63
La_N/Yb_N	9.08	4.05	7.24	8.47	8.03	6.82	7.18	7.60	8.79	6.77	7.49	7.52	6.94	6.49	6.72
La_N/Sm_N	5.19	2.90	3.93	2.91	3.08	2.97	3.26	3.23	4.25	2.63	4.26	4.18	4.27	4.48	3.75
Gd_N/Yb_N	1.05	1.07	1.18	1.77	1.58	1.23	1.39	1.62	1.25	1.43	1.07	0.96	0.91	0.87	1.06
CIA	77	74	76	76	76	76	76	77	79	78	72	72	72	71	73
PIA	95	99	98	99	99	98	98	97	99	99	99	99	99	99	98
CIW	96	99	99	99	100	99	99	98	99	99	99	99	99	99	99

Sample	KP14B	KP15A	KP15B	KP16A	KP17A	KP18A	KP18B	KP19A	KP19B	NP11	NP12	NP13	NP4	NP9	NP15
TiO_2	0.39	0.80	0.80	0.55	0.68	0.90	0.69	0.88	0.84	0.93	0.85	0.88	0.16	0.40	0.22
Al_2O_3	9.15	16.6	14.7	11.9	13.0	17.4	12.8	19.9	18.6	20.4	19.7	19.3	7.54	8.91	7.53
Fe_2O_3	1.30	2.26	2.25	1.50	1.39	6.79	2.21	1.91	4.04	7.05	6.61	8.46	1.02	2.61	0.79
MnO	0.01	0.01	0.01	0.01	0.01	0.01	0.01	0.01	0.01	0.01	0.02	0.22	0.00	0.00	0.00
MgO	0.62	1.18	1.07	0.78	0.82	1.13	0.81	0.22	0.23	0.71	1.75	1.51	0.36	0.56	0.36
CaO	0.01	0.01	0.01	0.01	0.01	0.01	0.01	0.01	0.01	0.02	0.01	0.01	0.01	0.01	0.01
Na_2O	0.03	0.08	0.06	0.06	0.09	0.13	0.10	0.38	0.33	0.45	0.34	0.40	0.01	0.01	0.01
K_2O	3.41	5.97	5.15	4.21	4.25	5.65	4.53	5.19	4.55	4.02	4.1	3.91	2.46	2.87	2.45
P_2O_5	0.01	0.02	0.01	0.02	0.02	0.02	0.02	0.03	0.04	0.10	0.05	0.08	0.02	0.03	0.03
LOI	1.70	2.91	2.76	2.20	2.57	3.81	2.48	3.72	3.69	5.30	4.17	4.80	1.15	2.16	1.52
Total	98.03	96.93	98.01	98.19	97.32	96.84	97.13	97.78	96.65	94.45	94.94	95.14	97.83	96.80	98.41
Rb	95.4	170	148	120	128	162	127	172	165	200	209	190	80.4	87.2	70.8
Sr	17.5	25.2	21.2	22.9	29.9	32.2	30.2	75.9	78.7	70.0	60.0	74.0	12.1	11.1	15.5
Ba	680	1050	892	651	772	789	622	875	840	579	647	591	275	819	284
Y	25.3	41.5	31.7	21.9	33.7	34.1	25.9	34.7	42.6	30.0	32.0	36.0	19.7	17.1	27.4
Zr	719	486	568	374	558	320	349	517	429	196	182	184	303	313	502
Hf	16.9	12.5	14.5	10.1	13.7	8.40	9.10	13.5	11.3	5.60	5.70	5.80	7.91	8.10	13.0
Nb	8.40	16.4	16.2	11.6	13.2	17.4	12.9	18.7	17.5	17.0	17.0	18.0	3.53	6.79	5.37

(*continued on next page*)

Table 1 (*continued*)

Sample	KP14B	KP15A	KP15B	KP16A	KP17A	KP18A	KP18B	KP19A	KP19B	NP11	NP12	NP13	NP4	NP9	NP15
Ta	0.60	1.20	1.20	0.80	1.00	1.20	1.00	1.40	1.30	1.50	1.50	1.40	0.25	0.56	0.37
Th	8.93	17.1	16.8	11.5	13.5	17.7	12.7	19.0	19.9	22.7	20.9	21.1	3.33	7.58	4.78
U	2.55	3.66	3.89	2.95	2.96	4.78	2.84	4.54	4.51	2.90	2.90	3.30	1.29	2.32	1.83
Sc	7	14	12	9	12	17	12	15	17	19	19	19	3	8	4
V	37	88	79	51	69	114	74	88	97	87	90	84	19	40	14
Cr	30	50	60	40	50	70	50	60	70	63	65	62	20	25	20
Co	2	4	2	1	1	3	2	1	0.99	3	14	22	3	3	2
Ni	3	9	8	5	10	10	4	8	3	8	21	22	10	10	8
Cu	2	4	3	3	1	38	10	12	19	18	21	32	9	32	9
La	28.8	60.7	37.2	33.4	44.4	35.3	32.4	42.6	46.0	50.5	50.5	56.6	19.3	20.2	20.0
Ce	65.3	140	76.0	73.3	101	87.1	68.1	77.8	92.1	106	112	131	47.9	37.5	46.8
Pr	7.21	16.7	8.51	8.08	11.2	9.87	7.74	8.28	10.6	10.9	11.4	13.6	5.43	3.51	5.26
Nd	27.7	67.3	31.9	30	44.3	39.1	28.4	29.6	41.7	39.6	42.3	51.7	21.1	12.2	21.2
Sm	4.92	13.0	5.79	5.32	8.79	7.90	5.07	5.52	8.03	7.70	8.30	10.2	4.24	2.29	4.75
Eu	0.93	2.20	1.11	0.99	1.59	1.30	1.01	1.10	1.21	1.34	1.41	1.81	0.93	0.48	1.03
Gd	4.32	9.60	4.73	4.09	7.51	6.34	4.01	5.32	7.89	6.10	6.40	8.20	4.22	2.37	5.19
Tb	0.66	1.37	0.79	0.63	1.11	0.99	0.69	0.90	1.26	1.00	1.10	1.30	0.66	0.46	0.91
Dy	4.34	7.72	5.87	3.91	6.45	6.37	4.84	6.09	7.93	6.00	6.50	7.30	3.72	2.93	5.17
Ho	0.93	1.59	1.22	0.88	1.29	1.32	0.98	1.30	1.60	1.20	1.30	1.40	0.68	0.60	0.99
Er	2.64	4.62	3.50	2.63	3.75	3.86	3.16	3.93	4.77	3.60	3.90	4.20	2.00	1.95	2.84
Tm	0.42	0.66	0.57	0.43	0.52	0.61	0.43	0.60	0.65	0.58	0.63	0.66	0.31	0.32	0.43
Yb	2.89	4.51	3.92	2.72	3.64	3.86	3.07	4.08	4.63	3.60	3.70	3.90	1.82	2.02	2.56
Lu	0.47	0.70	0.61	0.42	0.51	0.58	0.45	0.59	0.72	0.50	0.54	0.58	0.27	0.30	0.40
Eu/Eu*	0.62	0.60	0.65	0.65	0.60	0.56	0.68	0.62	0.46	0.60	0.59	0.60	0.67	0.63	0.63
La_N/Yb_N	6.68	9.02	6.36	8.23	8.18	6.13	7.07	7.00	6.66	9.40	9.15	9.73	7.11	6.70	5.24
La_N/Sm_N	3.65	2.93	4.01	3.92	3.15	2.79	3.99	4.82	3.58	4.09	3.80	3.46	2.85	5.49	2.63
Gd_N/Yb_N	1.21	1.73	0.98	1.22	1.67	1.33	1.06	1.06	1.38	1.37	1.40	1.70	1.87	0.95	1.65
CIA	71	72	72	72	73	73	72	76	77	80	80	80	74	74	74
PIA	99	99	99	99	98	98	98	96	96	96	96	96	100	100	100
CIW	99	99	99	99	99	99	99	97	97	96	97	97	100	100	100

reflect high intensity of source area weathering where K and Mg are fixed in clay minerals and Ca is preferentially leached (Fedo et al., 1996).

4.2. Large ion lithophile elements

The concentrations of the following elements; Ba, Rb, Cs, and Sr are in the range 156–1575 ppm, 24–210 ppm, 0.5–9.5 ppm and 9.5–205 ppm, respectively. Al_2O_3 shows positive correlations with Rb (r = 0.94), Sr (r = 0.60), Cs (r = 0.87), and Ba (r = 0.76) suggesting that these trace elements are associated with clay minerals and/or micas. There is strong positive correlation between K_2O and Rb (r = 0.87), and K_2O and Ba (r = 0.84), for the studied metasedimentary rocks suggesting that K-bearing clay minerals such as illite control the abundances of K, Ba and Rb (McLennan et al., 1983). No clear correlation exists between K_2O and Sr; however, Na_2O correlate with Sr (r = 0.82). Compared to average Neoproterozoic upper crustal values (normalization values from Condie, 1993) the studied metasedimentary rocks show strong depletion in CaO, Na_2O and Sr whereas K_2O, Rb and Ba are close to upper crustal concentrations (Fig. 4). Such geochemical signatures are typical of sedimentary rocks derived from intensively weathered source terrain where K, Rb and Ba are incorporated into clays during chemical weathering whereas Ca, Na and Sr are preferentially leached (Fedo et al., 1996).

4.3. Transition metals

The concentrations of the ferromagnesian trace elements Sc, V, Cr, Ni, Co range from 3 to 19 ppm, 14–118 ppm, 10–90 ppm, 3–24 ppm, and 1–25 ppm, respectively. The ferromagnesian trace element concentrations are generally lower in abundance than average Neoproterozoic upper crustal concentrations (Fig. 5). The trace elements Cr, Co, Ni, and V behave similarly during magmatic processes, though may be fractionated during weathering (Feng and Kerrich, 1990). Strong positive correlations exist among Sc, Cr and V and these elements also strongly correlates with Al_2O_3 (Table 3) suggesting that they were bounded in clays and concentrated during weathering (Asiedu et al., 2000; Fedo et al., 1996). However, Sc, Cr, and V do not show significant correlation with Ni and Co; positive correlation exists between Ni and Co (Table 3). Ni and Co show no such correlation with Al_2O_3 suggesting that the concentrations of these elements are largely controlled by oxides.

4.4. High field strength elements

The concentrations of Zr and Hf in the analysed metasedimentary rocks are between one and half to four times higher than those of upper crustal values (Fig. 5). The average Zr/Hf value of 38.9 is suggestive of zircon control (Zr/Hf ≈ 4.0) (Toulkeridis et al., 1999). Ti and Nb are positively correlated (r = 0.99) suggesting an ilmenite control (Toulkeridis et al., 1999). Th/U values are variable (2.32–7.83), and generally higher than that of the average Neoproterozoic upper crustal value of 3.8 (Condie, 1993). Th/Sc values are also variable (0.95–1.58) but higher than that of average Neoproterozoic upper crustal value of 0.71 (Condie, 1993).

4.5. Rare earth elements

The total rare earth element (ΣREE) abundances are highly variable (59.9–330, average ΣREE = 171; Table 1) and negatively correlates with SiO_2 contents (r = −0.8). The chondrite-normalized REE pattern displays a single general trend characterised by light-REE (LREE) enrichment (La_N/Sm_N, 5.49–2.63; average 3.68), significant negative europium anomaly (Eu/Eu*, 0.68–0.46; average 0.61) and fairly flat heavy-REE (HREE) (Gd_N/Yb_N, 1.87–0.86; average 1.3) (Fig. 6).

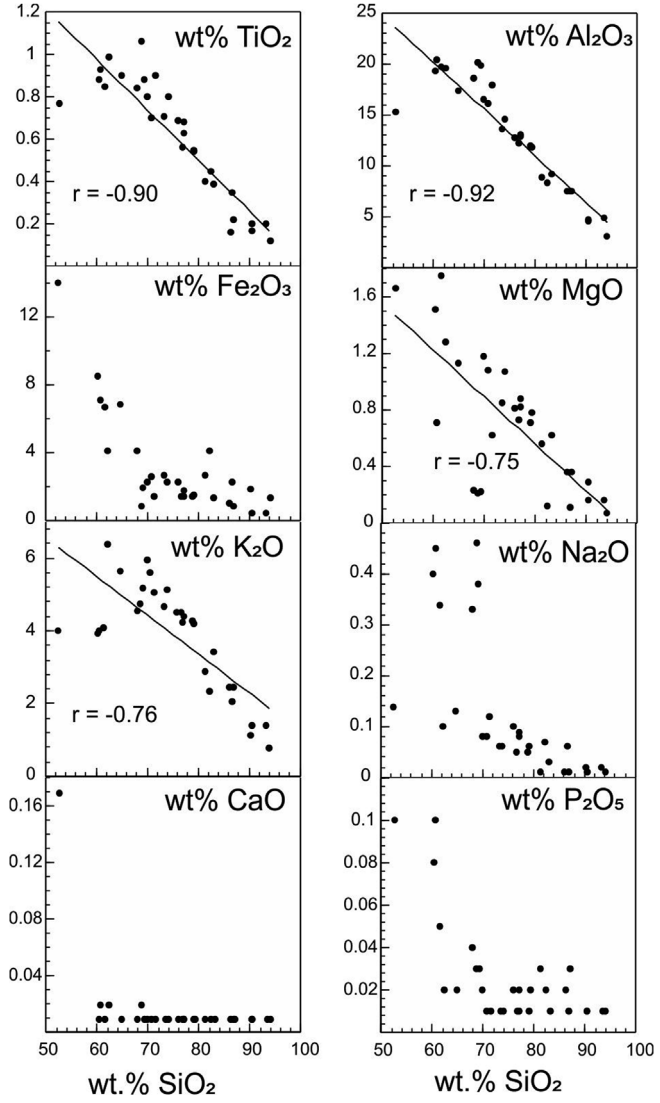

Fig. 3. Major oxides versus SiO_2 diagram for the Togo metasedimentary rocks.

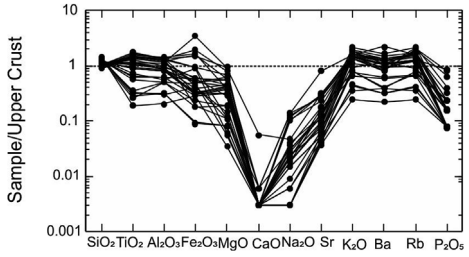

Fig. 4. A plot of phyllite samples from the TSU normalized against average juvenile upper crust (1.6–0.8 Ga), normalizing values from Condie (1993).

5. Discussion

5.1. Influence of Metamorphism

The Togo Structural Unit has undergone greenschist facies metamorphism. Several lines of evidence argue against large-scale remobilization of at least some elements in the analysed rock samples. All the analysed samples have fairly smooth REE patterns, which would not be expected during remobilization. In addition, the High field strength elements (e.g., Zr, Nb, Hf, Y) and ferromagnesian trace elements (Cr, Ni, V, Co, and Sc) generally show consistent inter-relationships (Table 3).

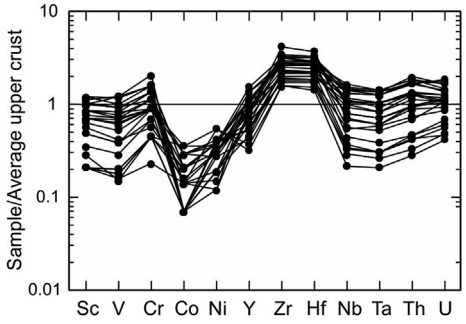

Fig. 5. Multi-element normalized diagram for the TSU metasedimentary rocks, normalized against average upper continental crust (Condie, 1993).

Table 2
Range of elemental ratios of TSU metasedimentary rocks in this study compared to the ratios of sediments derived from felsic and mafic rocks, and upper continental crust.

Elemental ratio	Range of metasedimentary rocks from TSU[a] (n = 30)	Range of sediments from felsic sources[b]	Range of sediments from mafic sources[b]	Neoproterozoic UCC[c]
Eu/Eu*	0.46 - 0.61	0.40 - 0.94	0.71 - 0.95	0.6
La/Sc	1.93 - 6.47	2.50 - 16.3	0.43 - 0.86	1.91
Th/Sc	0.89 - 1.58	0.84 - 20.5	0.05 - 0.22	0.71
La/Co	1.80 - 50.8	1.80 - 13.8	0.14 - 0.38	1.76
Th/Co	0.67 - 20.05	0.67 - 19.4	0.04 - 1.40	0.72
Cr/Th	2.78 - 6.00	4.00–15.0	25–500	4.46

UCC, Upper Contonental Crust.
[a] This study.
[b] Cullers et al. (1988), Cullers (1994, 2000) and Cullers and Podkovyrov (2000).
[c] Condie (1990).

These trace element relationships illustrate the chemical coherence and uniformity of the data and therefore argue against any large scale remobilization, at least for these elements.

Although it is possible that some elements such as large ion lithophile elements may have been remobilized, it is unlikely that large-scale remobilization of the REEs and the HFSE have occurred. Rather, other factors such as source area weathering and provenance must have played more important role in determining the distributions of these elements (Yang et al., 1998).

5.2. Source area weathering and metasomatism

The compositionally more complex clays such as smectites and chlorites, which contain Ca, Na, Fe, and Mn degrade quickly during weathering as compared to illite containing K_2O which is stable and resistant to weathering (Cox et al., 1995). Therefore, the relationship between these major elements may be used to infer the chemical weathering of sediments (Nesbitt and Young, 1982). The metasedimentary rocks of the TSU have high K_2O/Na_2O values (range = 8.93–113.67, average = 48.88) which support a high intensity of chemical weathering at the source area.

The intensity of chemical weathering of sedimentary and metasedimentary rocks can be quantified using indices proposed by various workers. One of such indices in the Chemical Index of Alteration (CIA) by Nesbitt and Young (1982) which measures the extent of conversion of feldspars to clays. CIA values of 50–60% indicate incipient weathering and values of 60–80% indicate moderate weathering whereas values greater than 80% indicate extreme weathering at the source area (Fedo et al., 1995). The studied metasedimentary rocks have relatively moderate to high CIA values (CIA = 71–80%; average = 75%) which are slightly higher than that of PAAS (70%; Taylor and McLennan,

Table 3
Pearson correlation coefficient among elemental pairs.

	SiO_2	Al_2O_3	Sc	V	Cr	Co	Ni	Cu	Rb	Sr	Cs	Ba	Y	Zr	Hf	Nb	Ta	Th	U	La
Al_2O_3	-.917**																			
Sc	-.935**	.960**																		
V	-.917**	.936**	.922**																	
Cr	-.862**	.926**	.901**	.945**																
Co	-.550**	.257	.365*	.281	.233															
Ni	-.416*	.166	.281	.198	.126	.865**														
Cu	-.311	.242	.367*	.196	.189	.284	.270													
Rb	-.899**	.974**	.952**	.894**	.858**	.255	.184	.250												
Sr	-.541**	.605**	.524**	.590**	.739**	.233	.087	.064	.445*											
Cs	-.835**	.866**	.921**	.753**	.754**	.401*	.291	.392*	.907**	.391*										
Ba	-.646**	.763**	.652**	.819**	.773**	-.020	-.102	-.044	.710**	.573**	.471**									
Y	-.815**	.823**	.790**	.816**	.817**	.281	.148	.153	.804**	.489**	.663**	.647**								
Zr	.196	-.052	-.178	-.036	.012	-.470**	-.573**	-.420*	-.066	-.053	-.240	.304	.213							
Hf	.123	.025	-.108	.028	.081	-.435*	-.545**	-.389*	.011	-.015	-.173	.352	.285	.993**						
Nb	-.894**	.972**	.937**	.947**	.951**	.237	.135	.180	.930**	.616**	.828**	.793**	.847**	.048	.122					
Ta	-.905**	.974**	.965**	.920**	.938**	.276	.192	.227	.947**	.609**	.881**	.720**	.821**	-.056	.017	.982**				
Th	-.919**	.964**	.972**	.905**	.926**	.329	.218	.277	.935**	.601**	.897**	.672**	.819**	-.083	-.011	.969**	.990**			
U	-.785**	.836**	.786**	.895**	.848**	.126	.022	.141	.784**	.452*	.585**	.789**	.819**	.264	.327	.890**	.818**	.802**		
La	-.822**	.857**	.854**	.776**	.813**	.388*	.238	.149	.824**	.615**	.820**	.620**	.793**	-.051	.012	.872**	.891**	.908**	.642**	
REE	-.802**	.808**	.824**	.746**	.771**	.415*	.262	.175	.796**	.524**	.804**	.553**	.831**	-.026	.035	.827**	.841**	.864**	.625**	.977**

*. Correlation is significant at the 0.05 level (2-tailed).
**. Correlation is significant at the 0.01 level (2-tailed).

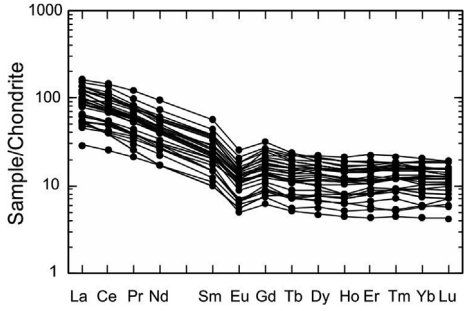

Fig. 6. Chondrite-normalized REE plots for the TSU metasedimentary rocks. Normalizing values from Taylor and McLennan (1985).

1985) and falls within the range for moderate chemical weathering.

During diagenesis, K− metasomatsism (i.e, illitisation of smectite and/or plagioclase albitization) leads to the addition of post-depositional potassium (K) to older clastic rocks (Fedo et al., 1995). This limits the use of the CIA parameter, which does not correct for this effect. The effect of K-metasomatism can be assessed from the position of the samples on the A−CN−K diagram (Fig. 7). The sample trend along the A-K line around illite, may suggest K addition from the conversion of highly aluminous clays, such as kaolinite to potassic clays such as illite resulting in the low CIA values (Fig. 7).

Accordingly, K− free indices such as plagioclase index of alteration (PIA) and the chemical index of weathering (CIW) have been calculated to determine the intensity of chemical weathering for the phyllites. The

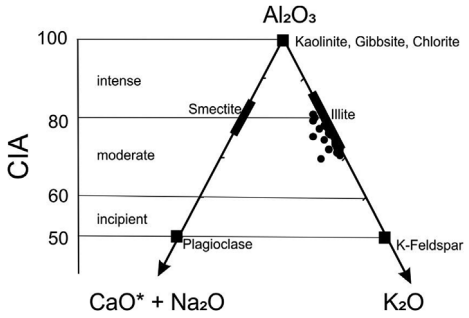

Fig. 7. A−CN−K diagram for the TSU metasedimentary rocks.

high PIA values (> 95%; Table 1) of the metasedimentary rocks indicate complete conversion of plagioclase into aluminous clay minerals such as kaolinite, illite and gibbsite (Fedo et al., 1995), suggesting high intensity of chemical weathering at source area. Again, the studied metasedimentary rocks have high CIW values (> 96%; Table 1) indicative of intense weathering at source area (Condie, 1993). Since the CIW values for the metasedimentary rocks are much higher than the CIA values, it is possible the studied samples might have experienced K-metasomatism.

5.3. Provenance of the metasedimentary rocks

The provenance of siliciclastic sedimentary rocks can be constrained using immobile trace elements, especially REEs, high field strength elements (HFSE) and the transition metals (Cr, Co, Ni, V and Sc). This is because the dispersion of HFSE and transition metals is not remarkably affected by sedimentary processes, diagenesis and metamorphism (Cox et al., 1995; McLennan, 1989; Taylor and McLennan, 1985; Wronkiewicz and Condie, 1987). Thus, in the discrimination of the provenance of the metasedimentary rocks of the TSU we make use of the immobile trace element data.

5.3.1. Composition of source areas

The elements La, Th, Co, and Sc are relatively immobile during weathering and metamorphism. Whereas La and Th are more concentrated in felsic than mafic igneous rocks, Co and Sc are more concentrated in mafic than felsic igneous rocks. Thus, ratios of La or Th to Co or Sc are sensitive indicators of source rock compositions (Cullers, 2000). Also, felsic igneous rocks typically contain negative Eu anomalies (Eu/Eu* from chondrite-normalized plots of the REE) whereas mafic igneous rocks contain little or no Eu anomalies (Cullers, 2000).

In Table 2, the provenance ratios deduced from composition of the analysed metasedimentary rocks have been compared with those from sediments derived from felsic and basic rocks as well as to the average Neoproterozoic upper crustal values (Condie, 1993). The TSU metasedimentary rocks show provenance ratios which are close to or within the range of sediments derived from felsic source rock.

Having discriminated felsic sources for the TSU metasedimentary rocks we now determine whether the source rocks were dominantly felsic igneous rocks or recycled sedimentary rocks. Sedimentary rocks derived predominantly from pre-existing sedimentary rocks are

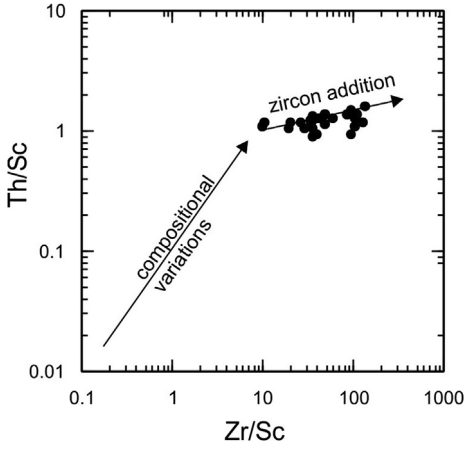

Fig. 8. Plot of Th/Sc versus Zr/Sc for metasedimentary rocks of the TSU (after McLennan et al., 1993).

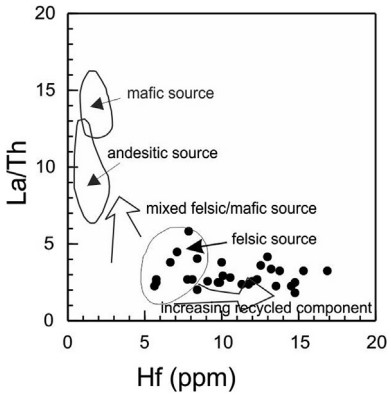

Fig. 9. Plot of La/Th versus Hf diagram (after Floyd and Leveridge, 1987).

characterised by zircon enrichment which can be reflected by relationships between Th/Sc and Zr/Sc (McLennan et al., 1993). On Th/Sc versus Zr/Sc diagram samples of sediments derived from igneous sources will follow the general provenance-dependent compositional variation trend whereas samples derived from recycled sedimentary source will follow the zircon addition trend (McLennan et al., 1993). On the Th/Sc versus Zr/Sc diagram, the TSU sandstones follow a trend suggestive of heavy mineral accumulation by sediment recycling and/or sorting (Fig. 8). The recycled or otherwise nature of source rocks can also be monitored on the La/Th versus Hf diagram (Floyd and Leveridge, 1987). On the La/Th versus Hf diagram the TSU metasedimentary rocks plot in the trend indicative of recycled sedimentary sources (Fig. 9). As an emphasis to the above, the observed enrichment of Zr and Hf in the analysed metasedimentary rocks relative to average Neoproterozoic upper crustal values (Fig. 5) suggests zircon accumulation and therefore supports the recycled nature of the metasedimentary rocks.

5.3.2. Location of source areas

Having inferred a recycled sedimentary provenance for the TSU metasedimentary rocks we now attempt to constrain the source areas for the metasedimentary rocks. Given that the metasedimentary rocks are Neoproterozoic in age, the only older sedimentary rocks presently exposed in Ghana and West Africa that are possible candidates for the supply of detritus to the TSU are the Paleoproterozoic Birimian sedimentary rocks (2000–2200 Ma; Abouchami et al., 1990; Boher et al., 1992; Hirdes et al., 1992; Taylor et al., 1992).

To evaluate this possibility, we compare the geochemical signatures of the metasedimentary rocks of TSU with those reported for the Birimian metasedimentary rocks. The geochemical characteristics of the Birimian metasedimentary rocks are significantly different from those of the TSU; the La/Sc, Th/Sc, La/Co, Th/Co ratios of the Birimian metasedimentary rocks are significantly lower than those observed in the metasedimentary rocks of the TSU (Asiedu et al., 2004, 2017). In addition, the Eu anomalies of the TSU metasedimentary rocks are significantly larger than those observed in the Birimian metasedimentary rocks (Asiedu et al., 2004, 2017). Therefore, the Birimian metasedimentary rocks, which may have been exposed for erosion, is unlikely to be the major source for the metasedimentary rocks of the TSU. Therefore, either the recycled sedimentary source for the TSU metasedimentary rocks have long been preferentially eroded, or the source is more distal, probably located outside the West African Craton.

Affaton et al. (1980) suggested that the TSU is a lateral equivalence of the Kwahu/Bombouaka Group of the Voltaian Basin. The geochemical characteristics of the analysed TSU metasedimentary rocks are very similar to those of the Bombouaka sandstones reported by Anani et al. (2017); both are K-rich, with Zr and Hf abundances higher than upper crustal values. In addition, their La/Sc, Th/Sc, La/Co, Th/Co ratios and Eu/Eu* values are similar. All of these geochemical similarities indicate that the TSU metasedimentary rocks and the sedimentary rocks of the Kwahu/Bombouaka Group may have a common recycled sedimentary source. This interpretation is supported by similar detrital zircon ages for both the TSU metasedimentary rocks and the sedimentary rocks of the Bombouaka Group (950–2200 Ma (TSU) and 1100–2200 Ma (Bombouaka Group); Kalsbeek et al., 2008) which overlap that of the Paleoproterozoic Birimian basement (2000–2200 Ma) underlying the Voltaian basin.

In summary, the geochemical data indicate that the metasedimentary rocks of the TSU were mainly derived from older recycled sedimentary rocks that are either no longer exposed in Ghana or of very distal origin. Previous studies have also shown that the rocks of the Togo Structural Unit include detrital zircon ages that are younger than ages observed in the Birimian rocks (Kalsbeek et al., 2008). According to Kalsbeek et al. (2008), these age ranges are typical of rocks deduced from sources beyond the West African Craton and probably from terrains within the Amazonian Craton.

5.3.3. Tectonic setting

The geochemical compositions of sedimentary rocks have been used to infer the tectonic settings of sedimentary basins; the application of immobile trace elements have particularly been useful (e.g., Bhatia and Crook, 1986). Although these discrimination diagrams were originally designed for Phanerozoic rocks they have been applied to Precambrian sedimentary rocks with some success (e.g., Holail and Moghazi, 1998; Yang et al., 1998).

According to Trompette (1997) and Caby (1998); Villeneuve and Cornée (1994), prior to the Pan-African Dahomeyide orogenic event, the southern margin of the West African Craton (WAC) rifted, followed by the opening of an oceanic basin. The subsequent formation of passive margins, experienced the sedimentation of clastics and carbonates. Later, there was an easterly subduction and eventual collision of the WAC with the Sahara-Meta Craton (Agbossomondé et al., 2004; Attoh, 1990; Attoh and Nude, 2008; Attoh et al., 1991) during the Pan-African orogenic event in southeastern Ghana. These interpretations are largely based on paleogeographic and geological location, lithology and deformational characteristics. In this study we attempt to discriminate the tectonic setting of the TSU metasedimentary rocks using the immobile trace element geochemistry of Bhatia and Crook (1986). On the ternary plot of La–Th–Sc (Fig. 10a), the TSU metasedimentary rocks dominantly plot within the continental margin (active and passive) with a few straddling around it but within the continental island arc. On the plots of Th–Co–Zr/10 (Fig. 10b), the TSU metasedimentary rocks plot predominantly within the passive margin with few plotting in and around the active continental margin. These plots suggest that continental materials dominated in the source.

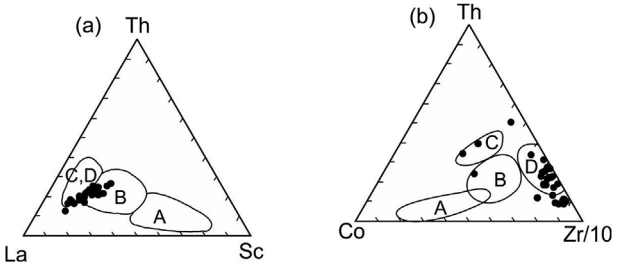

Fig. 10. Plots of TSU metasedimentary rocks on (a) La−Th−Sc ternary diagram and (b) Th−Co−Zr/10 ternary diagram.

The rocks of the Kwahu/Bombouaka Group are believed to have been deposited on a passive margin associated with the opening of a Pan-African ocean (Anani et al., 2017; Kalsbeek et al., 2008). Also, studies by Osae et al. (2006) showed that the rocks of Buem Structural Unit were of a passive margin origin. In this study, the provenance characteristics of the Togo phyllites indicate that the rocks were probably of a passive margin origin and to a lesser extent an active continental margin. These conclusions support the interpretation that the Kwahu/Bombouaka Group, Buem Structural Unit and Togo Structural Unit are lateral equivalents and were probably derived from the same source (Kalsbeek et al., 2008). The rocks of the Kwahu/Bombouaka Group, Togo Structural Unit and Buem Structural Unit reveal zircon ages of 1000–1300 Ma (Kalsbeek et al., 2008). From the geology of Ghana, no rocks of this age range had been observed in Ghana. According to Kalsbeek et al. (2008), these age ranges are typical of rocks deduced from sources beyond the West African Craton and probably from terrains within the Amazonian Craton. Considering the similar tectonic setting and depositional ages as well as the lateral correlation between the Kwahu/Bombouaka Group and the Togo Structural Unit, the rocks of the TSU were also probably derived from sources in the Amazonian Craton. According to Ganade deAraujo et al. (2016) the TSU and Bombouaka Group have detrital zircon ages similar with the flanking West Africa Craton that is comparable to that of the Martinópole Group in NE Brazil of the Amazonian Craton, taken as a direct correlative of the TSU.

6. Conclusions

The major-, trace-, and rare earth-element geochemistry of phyllites and phyllonites from the Togo Structural Unit which outcrop along the Akuapim range has been documented. The geochemical data yield several conclusions with regard to geochemical trends, provenance and tectonic settings, as summarized below:

1) CaO, Na_2O and Sr concentrations are significantly depleted with regard to average Neoproterozoic upper crust whereas K_2O, Rb and Ba are either enriched or close to upper crustal value. The high field strength elements and transition metals generally have Neoproterozoic upper crustal concentrations with exception of Zr and Hf that are significantly enriched with regard to average Neoproterozoic upper crust. The data show LREE enrichment, significant negative Eu anomaly and generally flat HREEs.
2) On the basis of immobile trace element ratios (i.e., La/Sc, Th/Sc, La/Co, Th/Co, Zr/Sc, La/Th ratios), Eu/Eu* values, and high Zr and Hf concentrations with regard to upper crustal values, the source rocks are believed to have composed predominantly of felsic recycled sedimentary rocks.
3) The metasedimentary rocks of the TSU have distinct geochemistry from the basement Birimian metasedimentary rocks, including large negative Eu anomalies and higher La/Sc, Th/Sc, La/Co, Th/Co, Zr/Sc ratios. The geochemical characteristics, however, are similar to the sedimentary rocks of the Bombouaka Group suggesting that they were derived from the same sources, probably in the Amazonian craton.
4) The metasedimentary rocks exhibit geochemical characteristics indicative of sediments derived from a passive continental margin. This inference supports previous studies which indicate that prior to the Pan-African Dahomeyide orogenic event, the southern margin of the West African Craton (WAC) was under passive margin settings.

Acknowledgement

Financial support for this work is provided by the Ministry of Lands and Natural Resources grant to the Department of Earth Science, University of Ghana (Earth Science Capacity Building Project).

Appendix A. Supplementary data

Supplementary data to this article can be found online at https://doi.org/10.1016/j.jafrearsci.2019.03.002.

References

Abouchami, W., Boher, M., Michard, A., Albarede, F., 1990. A major 2.1 Ga old event of mafic magmatism in West Africa: an early stage of crustal accretion. J. Geophys. Res. 95, 17605–17629.
Adjei, A.O., Tetteh, G.M., 1997. Deformational phases of the Togo series, Ho-Nyive-Honuta area, Ghana. Ghana Mining J. 3 (1 & 2), 1–9.
Adjei, A.O., 1968. The Structural Geology and Petrology of the Awudome-Abutia Area. MSc Thesis. University of Ghana, Legon, pp. 136.
Affaton, P., Rahaman, M.A., Trompette, R., Sougy, J., 1991. The Dahomeyide Orogen: tectonothermal evolution and relationships with the Volta basin. In: Dallmeyer, R.D., Lecorché, J.P. (Eds.), The West African Orogens and Circum-Atlantic Correlatives. Springer, New York, NY, pp. 95–111.
Affaton, P., Sougy, J., Trompette, R., 1980. The tectono-stratigraphic relationships between the upper precambrian and lower Paleozoic volta Basin and the Pan - African Dahomeyide orogenic belt (West Africa). Ame. J. Sci. 280, 224–248.
Agbossoumondé, Y., Guillot, S., Ménot, R.P., 2004. Pan-African subduction- collision event evidenced by high-P coronas in meta-norites from the Agou Massif (southern Togo). Precambrian Res. 135, 1–21.
Anani, C.Y., Mahamuda, A., Kwayisi, D., Asiedu, D.K., 2017. Provenance of sandstones from the neoproterozoic Bombouaka Group of the volta Basin, northeastern Ghana. Arabian J. Geosci. 10, 1–15. https://doi.org/10.1007/s12517-017-3243-2.
Asiedu, D.K., Suzuki, S., Nogami, K., Shibata, T., 2000. Geochemistry of lower Cretaceous sediments, Inner zone of Southwest Japan: constraints on provenance and tectonic environment. Geochem. J. 34, 155–173.
Asiedu, D.K., Dampare, S.B., Sakyi, P.A., Banoeng-Yakubo, B., Osae, S., Nyarko, B.J.B., Manu, J., 2004. Geochemistry of Paleoproterozoic metasedimentary rocks from the Birim diamondiferous field, southern Ghana: implications for provenance and crustal evolution at the Archean-Proterozoic boundary. Geochem. J. 38, 215–228.
Asiedu, D.K., Asong, S., Atta-Peters, D., Sakyi, P.A., Dampare, S.B., Anani, C.Y., 2017. Geochemical and Nd-isotopic compositions of juvenile-type Paleoproterozoic Birimian sedimentary rocks from southeastern West African Craton (Ghana): constraints on provenance and tectonic setting. Precambrian Res. 300, 40–52.
Attoh, K., 1990. Dahomeyides of Southeastern Ghana: Evidence for Oceanic Closure and Crustal Imbrication in a Pan-African Orogen. Publication Occasionnelle du C.I.F.E.G., BRGM, Orleans Tr. No. 21.
Attoh, K., 1998. High-Pressure Granulite facies metamorphism in the Pan-African Dahomeyide orogen, West Africa. J. Geol. 106 (2), 236–246.
Attoh, K., Nude, P.M., 2008. Tectonic significance of carbonatite and ultrahigh-pressure rocks in the Pan-African Dahomeyide suture zone, southeastern Ghana. Geol. Soc. Lond. Spec. Publ. 297, 217–231.
Attoh, K., Hawkings, G., Bowring, S.A., 1991. U-Pb zircon ages from the Pan-African Dahomeyide orogen, West Africa. EOS Trans. Am. Geophys. Union Spring. Meeting., Abstract, 72.
Ahmed, S.M., Blay, P.K., Castor, S.B., Coakley, G.J., 1977. Geology of field sheet 33, 59, 61 and 62. Winneba N. W. Accra S. W. N. W., and N. E., respectively. Ghana Geol. Surv. Bull. 32.
Bhatia, M.R., Crook, K.A.W., 1986. Trace elements characteristics of greywackes and tectonic setting discrimination of sedimentary basins. Contrib. Mineral. Petrol. 92, 181–193.
Black, R., Caby, R., Moussine-Pouchkine, A., Bertrand, J.M.L., Boullier, A.M., Fabre, J., Lesquer, A., 1979. Evidence for precambrian plate tectonics in West Africa. Nature 278, 223–227.
Black, R., Latouche, L., Li_egeois, J.P., Caby, R., Bertrand, J.M., 1994. Pan-African displaced terranes in the Tuareg shield (central Sahara). Geol 22, 641–644.
Boher, M., Abouchami, W., Michard, A., Albarede, F., Arndt, N.T., 1992. Crustal growth in West Africa at 2.1 Ga. J. Geophys. Res. 95, 345–369.
Caby, R., 1998. Tectonic history and geodynamic evolution of northern Africa during the Neoproterozoic. In: 14 International Conference on Basement Tectonics, Ouro Preto, pp. 72–75 Abstracts.

Condie, K.C., 1990. Growth and accretion of continental crust: inferences based on Laurentia. Chem. Geol. 83 (3-4), 183–194.
Condie, K.C., 1993. Chemical composition and evolution of the upper continental crust: Contrasting results from surface samples and shales. Chem. Geol. 104, 1–37.
Cordani, U.G., D'Agrella-Filho, M.S., Brito-Neves, B.B., Trindale, I.F., 2003. Tearing-up Rodinia: the neoproterozoic paleogeography of south American cratonic fragments. Terra. Nova 15, 350–359.
Cox, R., Lowe, D.R., 1995. A conceptual review of regional-scale controls on the composition of clastic sediment and the co-evolution of continental blocks and their sediment cover. J. Sediment. Res. A65 (1), 1–12.
Cox, R., Lowe, D.R., Cullers, R.L., 1995. The influence of sediment recycling and basement composition on evolution of mudrock chemistry in the southwestern United States. Geochim. Cosmochim. Acta 59 (14), 2919–2940.
Cullers, R.L., 1994. The controls on the major and trace element variation of shales, siltstones, and sandstones of Pennsylvanian-Permian age from uplifted continental blocks in Colorado to platform sediment in Kansas, USA. Geochim Cosmochim Acta. 58 (22), 4955–4972.
Cullers, R.L., 2000. The geochemistry of shales, siltstones and sandstones of Pennsylvanian Permian age, Colorado, USA: implications for provenance and metamorphic studies. Lithos 51, 181–203.
Cullers, R.L., Basu, A., Suttner, L.J., 1988. Geochemical signature of provenance in sand-size material in soils and stream sediments near the Tobacco Root batholith, Montana, USA. Chem. Geol. 70 (4), 335–348.
Cullers, R.L., Podkovyrov, V.N., 2000. Geochemistry of the Mesoproterozoic Lakhanda shales in southeastern Yakutia, Russia: implications for mineralogical and provenance control, and recycling. Precambrian Res. 104 (1-2), 77–93.
Dalziel, I.W.D., 1991. Pacific margins of Laurentia and East Antarctica–Australia as a conjugate rift pair: evidence and implications for an Eocambrian supercontinent. Geol 19, 598–601.
Dalziel, I.W.D., 1997. Neoproterozoic–Paleozoic geography and tectonics: review, hypothesis, environmental speculation. Geol. Soc. Ame. Bull. 109, 16–42.
Doblas, M., Lopez-Ruiz, J., Cebria, J.M., 2002. Mantle insulation beneath the west African craton during the precambrian-Cambrian transition. America 30 (9), 839–842.
Duodu, J.A., 2009. Ghana National Geological Map Project (Sheet 1:1000 000). Geological Survey Department of Ghana and Bundesanstalt fur Geowiessenschaften und Rohstoffe (BGR), Germany, pp. 1.
Ennih, N., Liégeois, J.P., 2008. The boundaries of West Africa craton, with a special reference to the basement of the Moroccan metacratonic Anti-Atlas belt. In: Ennih, N., Liégeois, J. p. (Eds.), The Boundaries of West Africa Craton. vol. 297. Geol. Soc. London, Spec. Pub, pp. 1–17.
Ennih, N., Liégeois, J.P., 2001. The Moroccan Anti-Atlas: the West African craton passive margin with limited Pan-African activity. Implications for the northern limit of the craton. Precambrian Res. 112, 289–302.
Fedo, C.M., Nesbitt, H.W., Young, G.M., 1995. Unravelling the effects of potassium metasomatism in sedimentary rocks and paleosols, with implications for paleo-weathering conditions and provenance. Geology 23, 921–924.
Fedo, C.M., Eriksson, K.A., Krogstad, E.J., 1996. Geochemistry of shales from the Archean (3.0 Ga) Buhwa Greenstone Belt, Zimbabwe: implications for provenance and source area weathering. Geochim. Cosmochim. Acta 60, 1751–1763.
Feng, R., Kerrich, R., 1990. Geochemistry of fine-grained clastic sediments in the Archean Abitibi greenstone belt, Canada: implications for provenance and tectonic setting. Geochim. Cosmochim. Acta 54, 1061–1081.
Floyd, P.A., Leveridge, B.E., 1987. Tectonic environment of the Devonian Gramscatho basin, south Cornwall: framework mode and geochemical evidence from turbidite sandstones. J. Geol. Soc. Lond. 144, 531–542.
Ganade de Araujo, C.E., Cordani, U.G., Agbossoumounde, Y., Caby, R., Basei, M.A.S., Weinberg, R.F., Sato, K., 2016. Tightening-up NE Brazil and NW Africa connections: NewU–Pb/Lu–Hf zircon data of a complete plate tectonic cycle in the Dahomey belt of the West Gondwana Orogen in Togo and Benin. Precambrian Res. 276, 24–42.
Grant, N.K., 1969. The precambrian to early Paleozoic orogeny in Ghana, Togo, Dahomey and Nigeria. Geol. Soc. Ame. Bull. 80, 45–55.
Griffis, R.J., Barning, K., Agezo, F.L., Akosah, F.K., 2002. Gold Deposits of Ghana. Minerals Commission publication, Accra, Ghana, pp. 37.
Hefferan, K.P., Admou, H., Karson, J.A., Saquaque, A., 2000. Anti-atlas (Morocco) role in Neoproterozoic western Gondwana reconstruction. Precambrian Res. 103, 89–96.
Hirdes, W., Davis, D.W., Eisenlohr, B.N., 1992. Reassessment of Proterozoic granitoid ages in Ghana on the basis of U/Pb zircon and monazite dating. Precambrian Res. 56, 89–96.
Hoffman, P., 1991. Did the breakout of Laurentia turn Gondwana inside out? Science 252, 1409–1412.
Holail, H.M., Moghazi, A.M., 1998. Provenance, tectonic setting and geochemistry of greywackes and siltones of the Late Precambrian Hammamat Group, Egypt. Sed.Geol. 116, 227–250.
Junner, N.R., 1940. The geology of the Gold Coast and western Togoland. Gold Coast Geol. Surv. Bull. 11, 1–40.
Junner, N.R., Service, H., 1936. Gold Coast geological survey annual report. 13, 32–34.
Junner, N.R., Hirst, T., 1946. The geology and hydrology of the Voltaian basin. Gold Coast Geological Survey Memoir 8, 51.
Kalsbeek, F., Frei, D., Affaton, P., 2008. Constraints on provenance, stratigraphic correlation and structural context of the Volta basin, Ghana, from detrital zircon geochronology: an Amazonian connection? Sediment. Geol. 212, 86–95.
Kalsbeek, F., Frei, R., 2010. Geochemistry of Precambrian sedimentary rocks used to solve stratigraphical problems: an example from the Neoproterozoic Volta basin, Ghana. Precambrian Res. 176, 65–76.
Kesse, G., 1985. The Mineral and Rock Resources of Ghana. In: Balkema, A.A. (Ed.), pp. 610 United States.
McLennan, S.M., 1989. Rare-earth element in sedimentary rocks: influence of provenance and sedimentary processes. Mineralogical Society of America. Reviews Mineral 21, 169–200.
McLennan, S.M., Taylor, S.R., Eriksson, K.A., 1983. Geochemistry of Archean shales from the Pilbara super group western Australia. Geochim. Cosmochim. Acta 47, 121–1222.
McLennan, S.M., Hemming, S., McDaniel, D.K., Hanson, G.N., 1993. Geochemical approaches to sedimentation, provenance and tectonics. In: In: Morton, A.C., Todd, S.P., Haughton, P.D.W. (Eds.), Development in Sedimentary Provenance, vol. 57. Geol. Soc. Ame. Spec. Publ., pp. 21–39.
Nesbitt, H.W., Young, G.M., 1982. Early Proterozoic climates and plate motions inferred from major element chemistry of lutites. Nature 299, 715–717.
Osae, O., Asiedu, D.K., Banoeng-Yakubo, B., Koeberl, C., Dampare, S.B., 2006. Provenance and tectonic setting of Late Proterozoic Buem sandstones of southeastern Ghana: evidence from geochemistry and detrital modes. J. Afri. Earth Sci. 44, 85–96.
Robertson, T., 1925. The sedimentary and volcanic rocks of western Togoland. Geol. Magazine 62 (1), 1–21.
Santos, J.O.S., Hartmann, L.A., Gaudette, H.E., Groves, D.I., Mcnaughton, N.J., Fletcher, I.R., 2000. A new understanding of the provinces of the Amazon craton based on integration of field mapping and U–Pb and Sm-Nd geochronology. Gond. Res. 3, 453–488.
Tassinari, C.G., Bettencourt, J.S., Geraldes, M.C., Macambira, M.J.B., Lafon, J.M., 2000. The Amazon craton. In: Cordani, U.G., Milani, E.J., Thomaz Filho, A., Campos, D.A. (Eds.), Tectonic Evolution of South America. Brazil, 31st Int. Geol. Congress, pp. 41–95.
Taylor, S.R., McLennan, S.M., 1985. The Continental Crust: its Composition and Evolution. Blackwell Science, pp. 312.
Taylor, P.N., Moorbath, S., Leube, A., Hirdes, W., 1992. Early Proterozoic crustal evolution in the Birimian of Ghana: constraints from geochronology and isotope geology. Precambrian Res. 56, 97–111.
Toulkeridis, T., Clauer, N., Kröner, A., Reimer, T., Todt, W., 1999. Characterization, provenance, and tectonic setting of fig tree greywackes from the Archaean Barberton greenstone belt, South Africa. Sediment. Geol. 124, 113–129.
Trompette, R., 1997. Neoproterozoic (600 Ma) aggregation of western Gondwana: a tentative scenario. Precambrian Res. 82, 101–112.
Villeneuve, M., Cornée, J.J., 1994. Structure, evolution and palaeogeography of the West African craton and bordering belts during the Neoproterozoic. Precambrian Res. 69, 307–326.
Villenenve, M., Dallmeyer, R.D., 1987. Geodynamic evolution of the mauritinide, bassaride and rokelide origens (West Africa). Precamb. Res. 37, 19–28.
Weil, A.B., Van der Voo, R., Mac Niocaill, C., Meert, J.G., 1998. The Proterozoic supercontinent Rodinia: paleomagnetically derived reconstructions for 1100 to 800 Ma. Earth Planet. Sci. Lett. 154, 13–24.
Wright, J., Hastings, D., Jones, W., Williams, H., 1985. Geology and Mineral Resources of West Africa. Springer, Netherlands, pp. 190.
Wronkiewicz, D.J., Condie, K.C., 1987. Geochemistry of Archean shales from the Witwatersrand Supergroup, South Africa: source area weathering and provenance. Geochim. Cosmochim. Acta 51, 2401–2416.
Yang, H., Kyser, K., Ansdell, K., 1998. Geochemical and Appendix A. Locations and mineralogical assemblages of the analysed samples Nd isotopic compositions of the metasedimentary rocks in the La Ronge Domain, Trans-Hudson Orogen, Canada: implications for the evolution of the domain. Precambrian Res. 92, 37–64.